Crystal Morphology Engineering by "Tailor-Made" Inhibitors: A New Probe to Fine Intermolecular Interactions

Z. Berkovitch-Yellin,* J. van Mil, L. Addadi,* M. Idelson, M. Lahav,* and L. Leiserowitz*

Contribution from the Department of Structural Chemistry, The Weizmann Institute of Science, Rehovot 76100, Israel. *Received August 23, 1984*

Abstract: A general method for the controlled modification of the morphology of organic crystals is described. The method comprises stereospecific inhibition of growth of preselected faces with the assistance of "tailor-made" growth inhibitors. The change in crystal habit is explained by a mechanism which takes into consideration a stereochemical correlation between the molecular structure of the additive, the crystal structure of the substrate, and the affected growth directions. The method has been successfully applied to primary amides ((*E*)-cinnamide, benzamide, *p*-toluamide, and *p*-clorobenzamide), carboxylic acids ((*E*)-cinnamic acid and benzoic acid), and steroids (androsterone and epiandrosterone). Dramatic changes in habit were induced by replacement, at the crystal surface, of a substrate N-H···O bond by an O···O repulsion, by replacement of an attractive C-H···O interaction by a C-H···H or C-Cl···O repulsion, or by insertion of a methyl or chlorine substituent instead of hydrogen, etc. The induced morphological modifications were used to obtain information on molecular interactions and conformations of the adsorbed inhibitor at the crystal surface. Thus, we could show that adsorbed additives benzamide and picolinamide assume twisted and planar conformations, respectively, on the affected faces of host benzoic acid, which is planar in the solid. In contradistinction, *p*-aminobenzoic acid tends to be planar when interacting with the growing faces of the nonplanar *p*-aminobenzamide. The additive (*E*)-cinnamide assumes a syn-planar C=C—C=O conformation on the affected surface of host (*E*)-cinnamic acid, which tends to assume an antiplanar C=C—C=O conformation. The effect of various additives on crystal habit is accounted for and quantitatively evaluated by atom-atom potential energy calculations.

Background. The morphology of a crystal is the result of the relative growth rates of its various faces, the general rule being that faces which grow slowest are expressed in the crystal habit. The growth rates of the different crystal faces are determined by intermolecular interactions between molecules in the crystal as well as by a number of external parameters such as solvent, supersaturation, temperature, and impurities. Changes in any of these may lead to dramatic modifications in crystal morphology. In particular, it is well established, both for inorganic and for organic crystals, that minute amounts of impurity, present in solution during crystallization, may induce morphological changes when selectively adsorbed at specific surfaces of the growing crystal.[1]

We have recently reported systematic studies on the effects on crystal habit caused by "tailor-made" additives whose molecular structures are very similar to those of the corresponding substrate molecules comprising the crystal.[2-6] The mechanistic information was derived from analyses of the relationship between the structure of the substrate crystal, the affected surfaces and the molecular structure of the additives.[2] We have deduced that the additive is selectively adsorbed at the host crystal sites only on those faces where its modified part emerges from the crystal surface. On these faces, the additive is bound in a very similar way to a substrate molecule by virtue of interactions between its unmodified part and the neighboring substrate molecules at the surface layer. Such an adsorbed guest molecule disturbs the regular deposition of oncoming crystal layers. This causes retardation of growth normal to these faces which generally leads to a relative increase in their surface area.

This approach has been exploited for the kinetic resolution of conglomerates,[2] the determination of the absolute direction of a polar axis in a crystal, the absolute configuration of both the chiral substrate[4] and the additive molecule,[5,6] the role of solvent on crystal growth,[7,8] and etch-pit formation upon dissolution of crystals in the presence of tailor-made additives.[9]

Objectives. In the present paper, we shall demonstrate that it is possible not only to explain observed morphological changes in crystals but rather to proceed in a reverse manner, namely to select inhibitors which will allow us to modify the habit of organic crystals in a desired and controlled manner. This method is general and applicable to organic materials of different nature and structure. It involves an analysis of the orientation of the molecules within the crystal, relative to its various faces, and the choice of appropriate additives which will bind at preselected faces and consequently inhibit growth in desired directions. The best predictions are made when the modifications on the substrate molecule are minor. We insert, for example, methyl or chlorine substituents instead of hydrogen atoms, generating steric hindrance. In other cases, hydroxyl oxygen atoms replace NH_2 groups of amides;[3] lone pair electrons are thus introduced at the sites of hydrogen atoms participating in H bonds, replacing NH···O attractive interactions by O···O repulsions. Twisted molecules substitute planar ones, or favorable C-H···O interactions[10] are replaced by C-H···H or C-Cl···O repulsions.

The effect of external parameters, like temperature, solvent, and supersaturation, are neutralized by crystallizing a specific substrate in the absence or presence of additives, under identical conditions except for the nature and concentration of the additive.

The principles of this approach are illustrated here for the crystallization of compounds of different chemical nature, i.e.,

(1) (a) Buckley, H. E. In "Crystal Growth"; Chapman and Hall: London, 1951. (b) Hartman, P. In "Physics and Chemistry of the Organic Solid State"; Fox, D., Labes, M., Weissberger, A., Eds.; Interscience: New York, 1963; Vol 1, Chapter 6. (c) Seifert, H. *Fortschr. Mineral. Kristallogr. Petrogr.* **1937**, *22*, 185. (d) Jetten, L. A. M. J.; van der Hoek, B.; van Enckevort, W. J. P. *J. Cryst. Growth* **1983**, *62*, 603.

(2) Addadi, L.; Berkovitch-Yellin, Z.; Domb, N.; Gati, E.; Lahav, M.; Leiserowitz, L. *Nature (London)* **1982**, *296*, 21.

(3) Berkovitch-Yellin, Z.; Addadi, L.; Idelson, M.; Lahav, M.; Leiserowitz, L. *Angew. Chem., Suppl.* **1982**, 1336. Preliminary results on the benzamide system were presented in this communication.

(4) Berkovitch-Yellin, Z.; Addadi, L.; Idelson, M.; Leiserowitz, L. Lahav, M. *Nature (London)* **1982**, *296*, 27.

(5) (a) Addadi, L.; Berkovitch-Yellin, Z.; Weissbuch, I.; Lahav, M.; Leiserowitz, L.; Weinstein, S. *J. Am. Chem. Soc.* **1982**, *104*, 2075. (b) Weissbuch, I.; Shimon, L. J. W.; Addadi, L.; Berkovitch-Yellin, Z.; Weinstein, S.; Lahav, M.; Leiserowitz, L. *Isr. J. Chem.*, in press.

(6) Weissbuch, I.; Addadi, L.; Berkovitch-Yellin, Z.; Gati, E.; Weinstein, S.; Lahav, M.; Leiserowitz, L. *J. Am. Chem. Soc.* **1983**, *105*, 6615.

(7) Berkovitch-Yellin, Z. *J. Am. Chem. Soc.*, in press.

(8) Wireko, F.; Berkovitch-Yellin, Z.; Frolow, F.; Lahav, M.; Leiserowitz, L., unpublished results.

(9) Shimon, L. J. W.; Lahav, M.; Leiserowitz, L. *J. Am. Chem. Soc.*, in press.

(10) Berkovitch-Yellin, Z.; Leiserowitz, L. *Acta Crystallogr., Sect. B* **1984**, *B40*, 159.

0002-7863/85/1507-3111$01.50/0

Table I. Strongest Intermolecular Interactions (kcal/mol) in (*E*)-Cinnamide Crystal: (A) between a Substrate (*E*)-Cinnamide Molecule and Neighboring (*E*)-Cinnamide Molecules; (B) between Additive Cinnamic Acid and Neighboring (*E*)-Cinnamide Molecules (*E*, Electrostatic Energy; *U*, van der Waals Energy)

neighbor site,[a] $a_1a_2a_3$	neighbor symmetry[b]	A			B		Δ(B-A)	
		E	*U*	*E* + *U*	*E*	*E* + *U*	*E* + *U*	description
211	3	−10.1	−1.7	−11.7	−6.0	−7.3	4.4	H-bonded dimer
$0\bar{1}0$	1	−6.2	−5.0	−11.2	0.5	−3.8	7.4	NH···O bond
010	1				−3.0	−8.2	3.1	along the *b* axis
$1\bar{1}0$	2	−0.7	−6.1	−6.8	−1.4	−7.3	−0.5	stacking
100	2				−0.5	−6.5	0.3	energy
111	3	2.2	−8.6	−6.3	1.7	−6.9	−0.6	close-packed pair

[a] The site of the neighboring molecule is described by the lattice vector $V = a_1a + a_2b + a_3c$ and the space group symmetry operator[b]. [b] (1) *x*,*y*,*z*; (2) $-x, {}^1/_2 + y, {}^1/_2 - z$; (3) $-x,-y,-z$; (4) $x, {}^1/_2, -y, {}^1/_2 + z$.

primary amides, carboxylic acids, and steroids each grown in the presence of various tailored additives.

For the first systems presented in this paper, cinnamide and benzamide,[3] we describe the application of the method for the modification of the crystal morphology in each of the three principal crystallographic directions, exploiting different intermolecular interactions which exist in the crystal lattice of the substrate.

Having established the direct relationship between the change in crystal habit and the molecular structure of the inhibitor, we proceed to exploit the modified crystal morphology in order to obtain information on molecular interactions and conformations of the inhibitor molecules at the surface and inside the bulk of the substrate crystal.

Theoretical Methodology. The effect of various additives on crystal habit is accounted for and quantitatively evaluated by atom–atom potential energy calculations, undertaken to understand the crystal habit in terms of its structure and of specific intermolecular interactions, as well as to pinpoint the nature of host–additive interactions which are responsible for the change in habit.

The calculated intermolecular interactions[11] in the crystals are used for the derivation of the layer energy (E_l) and attachment energy (E_{att}) of various faces. E_l, which is defined[13a] as the energy per molecule released when a new layer is formed, measures the stability of the faces. E_{att}, which is defined as the energy per molecule released when a layer is attached to the crystal, is proportional to the growth rate normal to the face. The "theoretical form", which was derived from E_{att} of various stable crystal faces,[13b] was found to be in nice agreement with observed crystal habits grown by sublimation.[7]

These calculations were further extended for the prediction of the effect of additives on crystal habit. To establish the exact faces which are expected to be modified by specific additives, we look for those faces which would bind the additive with a relatively low loss in binding energy. Thus, we calculated differences in binding energy (ΔE_b) of the additive, relative to the pure substrate molecule at various crystallographic sites on different crystal faces. The binding energy at the surface site was defined as the sum $E_{att} + E_l$. $\Delta E_b = E_b - E_b'$, where E_b and E_b' are the binding energies of the substrate and additive, respectively. The latter is obtained from E_{att}' and E_l', which are the attachment and layer energies calculated with reference to an additive molecule.[7]

In most of these calculations we assume that the additive adopts a conformation which is similar to that of the substrate molecules and thus is bound at a substrate molecular site with similar interactions as a substrate molecule, except for that part of the additive which is modified with respect to the substrate.

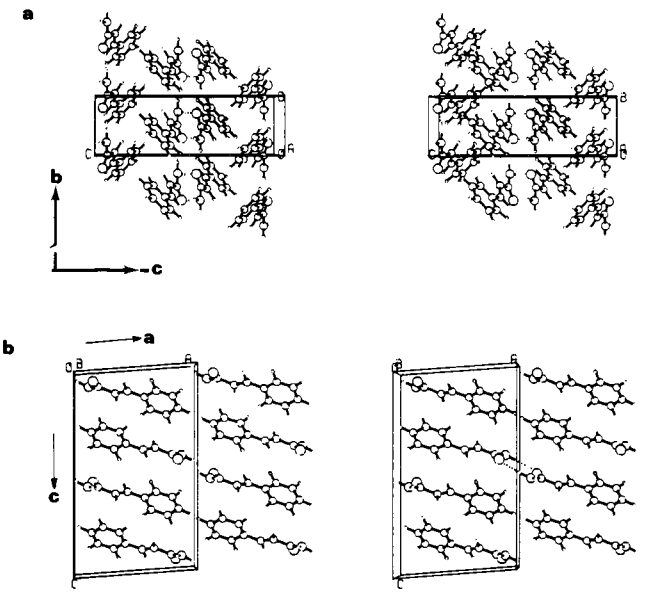

Figure 1. Packing arrangement of (*E*)-cinnamide (a) as viewed along the *a* axis and (*b*) as viewed along the *b* axis.

Results

1. Primary Amides. 1.1. (*E*)-Cinnamide crystallizes from ethyl acetate in space group $P2_1/c$ as bars extended along the *b* axis, with principal faces {001}, {100}, {011}, and {102} (Figure 2a).[14]

Within the crystal[15] (Figure 1) (*E*)-cinnamide molecules form H-bonded cyclic dimers in the direction of the *a* axis. These dimers are interlinked by NH···O hydrogen bonds of −11 kcal/mol (Table I) along the *b* axis to form a ribbon motif. The ribbons are interleaved along *c*, generating centrosymmetric molecular pairs which form plane-to-plane contacts of approximately 4 Å.

A decrease in the growth rate along *a* may be conceivably achieved either by disruption of the H bonds within the cyclic dimer, at the site of the additive, or by weakening the interactions between the stacked phenyl groups.

N-Methyl-(*E*)-cinnamide (**1**) and *p*-chlorocinnamide (**3c**) were consequently tested as suitable additives. Both cause cinnamide to grow as thin {100} plates (Figure 2b). The *N*-methyl group

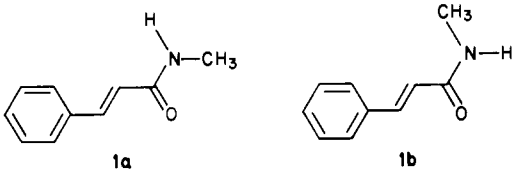

1a **1b**

of the additive molecule, which invariably adopts the O=C—

(11) The energy function used for the calculations included van der Waals and electrostatic terms. The latter were derived from experimental deformation electron density distributions. Similar functions have been successfully applied for analyzing packing characteristics of various polar and nonpolar molecules.[10,12]

(12) (a) Berkovitch-Yellin, Z.; Leiserowitz, L. *J. Am. Chem. Soc.* **1980**, *102*, 7677. (b) Berkovitch-Yellin, Z.; Leiserowitz, L. *J. Am. Chem. Soc.* **1982**, *104*, 5052. (c) Berkovitch-Yellin, Z.; Ariel, S.; Leiserowitz, L. *J. Am. Chem. Soc.* **1983**, *105*, 765.

(13) (a) Hartman, P.; Perdok, W. G. *Acta Crystallogr.* **1955**, *8*, 49. (b) Hartman, P.; Bennema, P. *J. Cryst. Growth* **1980**, *49*, 145.

(14) The symbol {} indicates all symmetry-related faces; ( ) indicates just the given face.

(15) (a) Leiserowitz, L.; Schmidt, G. M. J. *J. Chem. Soc., A* **1969**, 2372. (b) Wang, J. L., unpublished results.

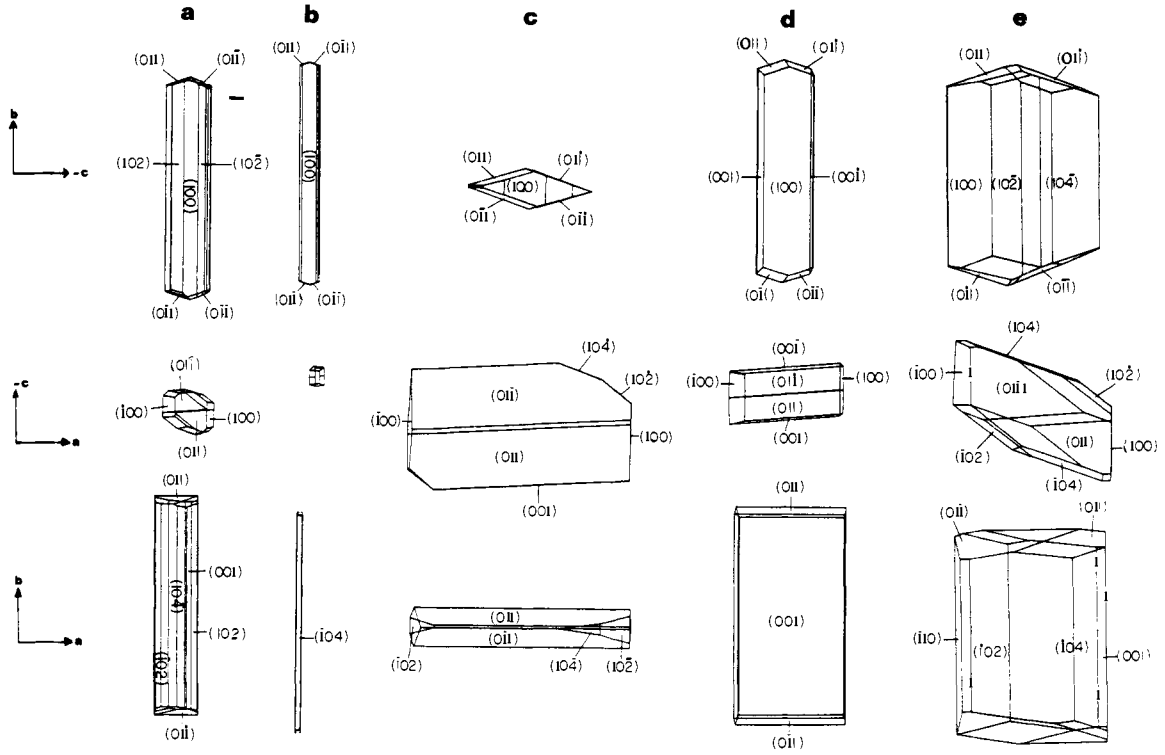

Figure 2. Crystals of (*E*)-cinnamide grown in the absence and presence of additives, viewed along the *a*, *b*, and *c* axis, respectively: (a) pure; (b) + *N*-methyl-(*E*)-cinnamide or *p*-chloro-(*E*)-cinnamide; (c) + (*E*)-cinnamic acid; (d) + α- or β-chloro-(*Z*)-cinnamide; (e) + *o*-chloro-(*E*)-cinnamide.

N—CH_3 syn conformation (**1a**),[16] prevents the formation of the dimer, thus inhibiting attachment of additional cinnamide molecules along *a*.

In the case of the additive *p*-chlorocinnamide, the bulky chlorine atom at the para position inhibits the deposition of oncoming 100 layers due to steric hindrance.

The driving force for growth of the crystal in the *b* direction is the energy released by formation of the N-H···O hydrogen bonds of the ribbon motif.[15] (*E*)-Cinnamic acid can replace an (*E*)-cinnamide molecule at the end of the ribbon; however, at the site of the additive, the attractive NH···O interaction is replaced by a repulsion between the adjacent oxygen lone pair electrons of the bound additive molecule and of the on-coming cinnamide molecule (Scheme I). This repulsion causes inhibition of growth along *b*. We assume here that the occluded cinnamic acid adopts the commonly observed[17] O=C—O—H syn-planar conformation (**2a**), as opposed to anti-planar one (**2b**). This assumption was

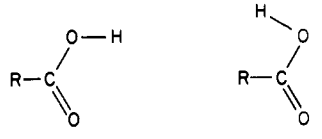

2a **2b**

substantiated by energy calculations of a similar substrate/additive system, benzamide/benzoic acid (see section 1.2) and has been demonstrated by low-temperature X-ray diffraction studies in another analogous system, asparagine-aspartic acid.[18]

As predicted, the presence of cinnamic acid in solution causes a drastic decrease in the growth rate of cinnamide crystals in the *b* direction, yielding flat prisms with prominent {011} faces (Figure 2c).

The crystal morphology was modified along *c* by the use of amide additives which contain bulky Cl substituents at the α- or β-carbon atoms of cinnamide. When a substrate molecule is

Scheme I

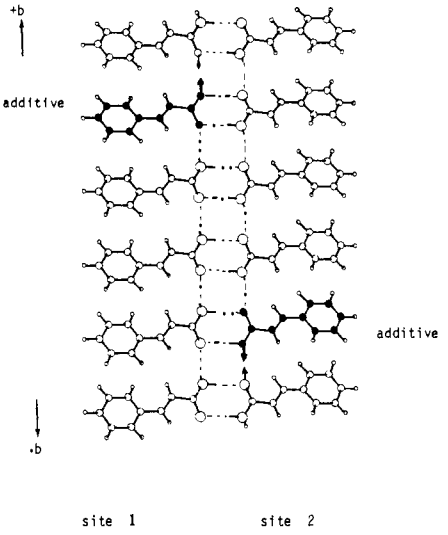

substituted, these additives interfere with the deposition of the next 001 layers (Figure 1). Indeed, crystallization of cinnamide in the presence of α- or β-chlorocinnamide (**3e** or **3d**) results in the separation of platelike crystals with prominent {001} faces (Figure 2d). *o*-Chlorocinnamide (**3a**, **b**)[19] has a similar effect

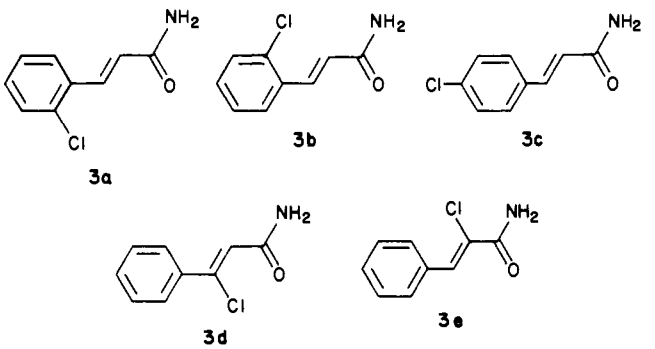

3a **3b** **3c**

3d **3e**

(16) Leiserowitz, L.; Tuval, M. *Acta Crystallogr., Sect. B* **1978**, *B34*, 1230.
(17) Leiserowitz, L. *Acta Crystallogr., Sect. B* **1976**, *B32*, 775.
(18) (a) Wang, J. L.; Berkovitch-Yellin, Z.; Leiserowitz, L. *Acta Crystallogr., Sect. B*, in press. (b) Wang, J. L. M.Sc. Thesis, submitted to the Feinberg Graduate School, Weizmann Institute of Science, May 1983.

Table II. (*E*)-Cinnamide: Layer Energy (E_l, kcal/mol) and Differences in Binding Energy (E_b, kcal/mol) of Various Additives Inserted at each of the Four Different Surface Sites[a] on Some Stable Faces of Cinnamide: (A) (*E*)-Cinnamic Acid, (B) *o*-Cl-(**3a**), (C) *o*-Cl-(**3b**), (D) *p*-Cl-(**3c**), (E) β-Cl-(**3d**), (F) hypothetical α-Chloro-(*Z*)-Cinnamide (**3e**)

face	E_l	site	A	B	C	D	E	F
(100)	−53.8	1	12.4	189.0	268.0	93.7	182.0	120.4
		2	13.9	189.0	272.0	−2.1	180.0	118.9
		3	13.8	189.0	268.0	−2.5	180.0	119.1
		4	12.3	189.0	268.0	94.2	182.0	120.4
(002)[c]	−51.5	1	13.4	189.0	267.0	93.7	181.0	119.4
		2	13.3	189.0	−1.1	−2.7	181.0	0.4
		3	13.2	189.0	−1.1	−2.7	181.0	0.5
		4	13.4	189.0	268.0	94.3	181.0	119.6
$(10\bar{2})$	−50.1	1	13.9	189.0	268.0	93.7	181.0	120.0
		2	13.8	−2.3	272.0	−2.3	−3.8	119.6
		3	13.6	−2.0	268.0	−2.3	−3.5	119.9
		4	13.7	188.0	268.0	94.1	181.0	120.1
(202)[c]	−39.2	1	12.0	−2.1	268.0	94.0	−2.1	121.3
		2	13.5	189.0	272.0	−2.0	180.0	118.6
		3	13.3	189.0	268.0	−2.2	181.0	118.9
		4	12.0	−1.8	267.0	94.5	−2.0	121.4
(102)	−36.5	1	12.3	190.0	268.0	93.8	182.0	120.2
		2	13.4	190.0	−1.1	−1.6	182.0	0.6
		3	13.2	189.0	−1.0	−1.7	182.0	0.7
		4	12.4	189.0	268.0	94.4	182.0	120.4
$(20\bar{2})$[c]	−36.0	1	11.9	190.0	−0.8	94.6	183.0	1.9
		2	13.8	189.0	272.0	−2.2	180.0	118.8
		3	13.6	189.0	268.0	−2.4	180.0	119.0
		4	11.8	189.0	−0.6	94.9	183.0	1.9
$(10\bar{4})$	−35.6	1	13.6	189.0	−0.8	94.8	182.0	1.8
		2	13.6	−2.2	272.0	95.2	−2.9	120.3
		3	13.4	−1.8	268.0	95.1	−2.7	120.5
		4	13.4	189.0	−0.6	95.0	182.0	1.8
(011)	−33.7	1	10.7	−2.0	268.0	95.2	−3.6	119.7
		2	10.3	−2.4	271.0	26.2	−3.6	120.1
		3	7.4	189.0	−2.9	64.5	181.0	−2.4
		4	6.4	189.0	268.0	94.4	181.0	117.1
(004)[d]	−29.8	1	13.4	−1.8	268.0	94.0	−2.1	120.4
		2	13.3	189.0	−1.1	−2.8	181.0	0.4
		3	13.2	189.0	−1.1	−2.7	181.0	−0.5
		4	13.4	−1.5	268.0	94.4	−2.0	120.5

[a] (1) x,y,z; (2) $-x,{}^1/_2+y,{}^1/_2-z$; (3) $-x,-y,-z$; (4) $x,{}^1/_2-y,{}^1/_2+z$. [b] $E_{crystal} = E_l + 2E_{att} = -74.6$ kcal/mol. [c] Halving of some layers is done because of space group symmetry $P2_1/c$. [d] The crystal has a natural (004) layer of spacing half that of (002).

but influences predominantly the growth of the $\{10\bar{4}\}$ faces, which form a small dihedral angle with the {001} faces (Figure 2e).

We further investigated the effects of a number of additives which are modified in more than one molecular site with respect to the substrate molecule. The results and the implications thereof are described in the discussion.

The effect of (*E*)-cinnamic acid and various Cl derivatives of (*E*)-cinnamide (**3a**–**3e**) was studied by energy calculations.

In order to quantitatively evaluate the effect of the additive (*E*)-cinnamic acid, we compare (in Table I) the substrate/substrate and substrate/additive intermolecular interactions. The largest loss in energy at the site of the acid additive is along the *b* axis. The loss of 7.4 kcal/mol is composed of two contributions, the disruption of an NH···O hydrogen bond of 6 kcal/mol[12a] and the insertion of an O···O repulsion of 1–2 kcal/mol. The difference of 4.4 kcal/mol in the energy of the hydrogen-bonded dimer amide/acid, relative to that of the amide/amide, originates from the fact that the amide oxygen atom is a much stronger proton acceptor than the corresponding carboxyl oxygen atom.[12]

Table II summarizes differences in binding energy of the additives on various stable faces of cinnamide. From the table it is clear that cinnamic acid,[20] in the syn-planar conformation (**2a**), is most easily adsorbed at two sites on the {011} faces of cinnamide, with an average loss in energy of 7 kcal/mol. This loss in energy does not originate from repulsive substrate/additive interactions but primarily from the fact that the acid/amide dimer at the site of the additive is less stable than the amide/amide dimer. The adsorbed cinnamic acid interferes with on-coming cinnamide molecules, due to O(acid)···O(amide) repulsion. This is reflected by the calculated loss in attachment energy (ΔE_{att}), which is maximal for these faces. This result is in accordance with the observation that the morphological importance of the {011} faces is dramatically increased when (*E*)-cinnamide is grown in the presence of (*E*)-cinnamic acid. The {010} faces, which might be expected to form in terms of ease of adsorption, cannot be developed because they are not stable[7] (see Discussion section).

In the case of the Cl derivatives, the additive was assumed to adopt a conformation akin to that of cinnamide but for the substitution of the relevant C–H bond by a C–Cl bond of 1.75 Å. However, for α-chlorocinnamide (**3e**), such conformation is unreasonable due to a short $Cl\cdots H_{ortho}$ intramolecular contact of 2.2 Å, and an additional torsion must be assumed. According to Table II, the various Cl derivatives are predicted to induce two distinct morphological modifications of cinnamide crystals: *o*-, α-, and β-chlorocinnamide, should affect the $\{10\bar{l}\}$ faces ($l \neq 0$) and specifically {001} which has a large morphological importance in pure (*E*)-cinnamide crystals, thus converting the crystals into {001} plates. *p*-Chlorocinnamide should affect primarily {100} and {001},

(19) *o*-Chlorocinnamide and *o*-chlorocinnamic acid have two possible molecular conformations, (**3a**) or (**3b**), which differ in the orientation of the *o*-Cl substituent with respect to the vinyl group. However, the conformation having the *o*-Cl substituent syn to the vinyl group (**3b**) is expected to be less stable due to the proximity of the chloride atom to the vinyl proton. As the exact conformation of *o*-chlorocinnamide is not known, the effect of both conformers (**3a**) and (**3b**) on the habit of (*E*)-cinnamide crystals was studied by energy calculations.

(20) (a) The occluded acid additive molecule was assumed to adopt a nonplanar conformation similar to that of substrate amide molecules. The geometry of the amide/acid hydrogen-bonded dimer was taken to be similar to that of a comparable amide/acid dimer found in the structure of fumaramic acid.[20b] (b) Hirshfeld, F. L. *Acta Crystallogr., Sect. B* **1971**, *B27*, 769.

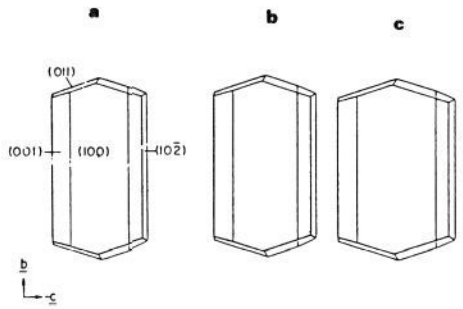

Figure 3. "Theoretical form" of solid solutions of c% (*E*)-cinnamic acid in (*E*)-cinnamide crystals: (a) c = 0%; (b) c = 20%; (c) c = 50%.

Table III. (*E*)-Cinnamide: Effective Attachment Energies (kcal/mol) of Various Stable Faces of the Solid Solutions (*E*)-Cinnamide/(*E*)-Cinnamic Acid for Various Concentrations [c] of the Acid

face	c, %					
	0	10	20	40	50	del[a]
(100)	−10.54	−10.31	−10.20	−9.96	−9.84	0.70
(002)[b]	−11.54	−11.52	−11.52	−11.47	−11.42	0.12
(10$\bar{2}$)	−12.22	−12.27	−12.29	−12.34	−12.37	0.15
(202)[b]	−17.72	−17.52	−17.33	−16.95	−16.77	0.95
(102)	−16.92	−16.78	−16.63	−16.34	−16.20	0.72
(20$\bar{2}$)[b]	−19.31	−19.16	−19.05	−18.97	−19.00	0.31
(10$\bar{4}$)	−19.49	−19.45	−19.42	−19.36	−19.33	0.16
(011)	−20.45	−19.55	−18.71	−17.27	−16.66	3.76

[a] del = $E_{eff}(50) - E_{eff}(0)$. [b] Halving of some layers is done because of space group symmetry $P2_1/c$.

which are the most prominent faces of cinnamide; thus needles elongated in b were expected. The experimental observation that *p*-chlorocinnamide induces the formation of thin {100} plates is probably due to the differences in the energies of the two {100} and {001} faces, since the additive can be adsorbed on both. These results are in good agreement with the experimentally observed morphologies.

Amounts of the (*E*)-cinnamic acid additive of 0.2–0.5% were typically found occluded in the bulk of the cinnamide crystal, even when the amount of the additive in solution was as high as 10% w/w of substrate. Moreover, it was found that the morphological effect of cinnamic acid on cinnamide increases gradually with increasing additive concentrations, even for acid concentrations at which the amount of occluded additive was not further increased. This possibly points to the importance of inhibitor molecules that only temporarily reside on the growing crystal surface and are eventually ejected into the solution before growth is resumed.

In an attempt to simulate the gradual change of the habit of cinnamide crystals in the presence of increasing amounts of cinnamic acid and to determine the effective amount of cinnamic acid which is needed to reproduce the observed morphological importance of various faces of cinnamide crystals, we have calculated E_{att} of various faces of the solid solutions of cinnamic acid in cinnamide crystals. The calculations were performed for a pure cinnamide crystal (E_1), an acid molecule surrounded by amide molecules (E_2), an amide molecule surrounded by acid molecules (E_3), and acid molecules surrounded by acid molecules (E_4). The effective E_{att} (E_{eff}) of various crystal faces as a result of [c]% cinnamic acid adsorbed at the growing sites was calculated by the expression

$$E_{eff}(c) = (1 - c)^2E_1 + c(1 - c)(E_2 + E_3) + c^2E_4$$

Table III lists E_{eff} for various crystal faces for concentrations [c] in the range of 0–50%. From the table it is clear that the main change in E_{att}, and thus in the growth rate, is for the (011) face, on which the additive was found to adsorb with a minimal loss in energy (Table II). The habit of cinnamide which was calculated by using the various E_{eff}[7] showed the expected tendency—an increase in the area of {011} (Figure 3). However, the effect was not as dramatic as the observed. This indicates that the solid solution model is not appropriate for a quantitative evaluation of the morphological changes, primarily because it assumes that the influence of the additive is proportional to its concentration. It has been shown that in fact minute amounts of inhibitor may already cause a drastic decrease in the rate of growth of the affected face.[1d]

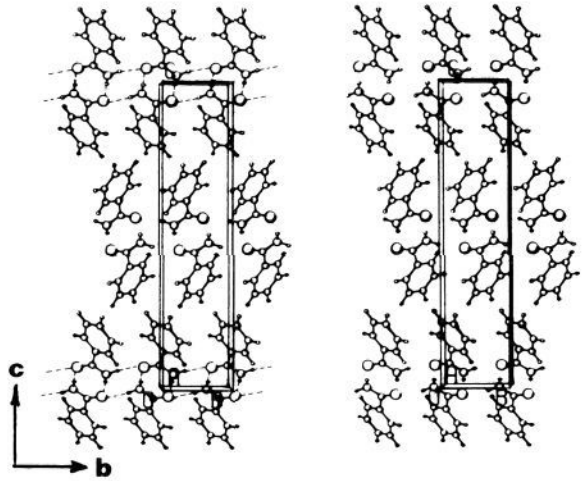

Figure 4. Packing arrangement of benzamide as viewed along the a axis.

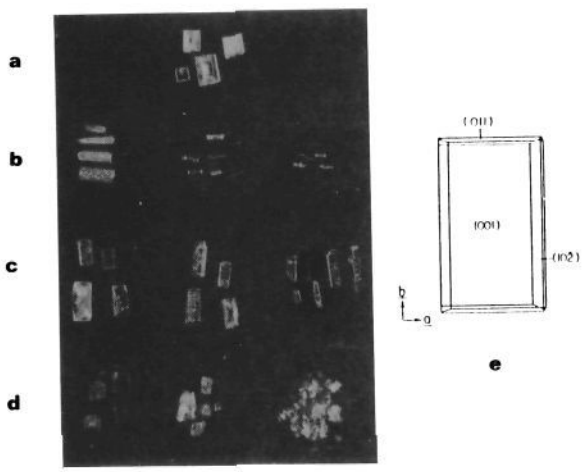

Figure 5. Crystals of benzamide grown in the absence and in presence of increasing amounts (from left to right) of additives, as viewed along the c axis: (a) pure; (b) + benzoic acid (3%, 5%, 10%); (c) + *o*-toluamide (1%, 5%, 10%); (d) + *p*-toluamide (1%, 3%, 5%); (e) computer-drawn picture of a typical benzamide crystal.

1.2. Benzamide crystallizes from ethanol in space group $P2_1/c$, as rectangular {001} plates extended in b (Figure 5a).

The main features of the crystal structure[21] (Figure 4) are similar to those found in cinnamide. Hydrogen-bonded cyclic dimers are interlinked along the 5.0-Å b axis to form ribbons of energy −22 kcal/mol. The ribbons are stacked along the 5.6-Å a axis with a stabilization energy of −13 kcal/mol, which is primarily due to van der Waals interactions. The ribbon and stack motifs combine to yield stable 001 layers. These tightly packed layers juxtapose along the c axis by weaker van der Waals contacts between phenyl groups (−9 kcal/mol). From these energies, it is clear that the primary directions of growth are along the b and a axes, and the growth along c is the slowest, thus explaining the {001} platelike shape of the crystals.

Reasoning as for cinnamide, additives *p*-toluamide, benzoic acid, and *o*-toluamide were selected to inhibit growth along the a, b, and c axes, respectively.[3] The resulting crystal morphologies are shown in Figure 5.

(21) Blake, C. C.; Small, R. W. *Acta Crystallogr., Sect. B* **1972**, *B28*, 2201.

Table IV. Benzamide: Layer Energy (E_l, kcal/mol) and Differences in Binding Energy (E_b, kcal/mol) of Various Additives Inserted at each of the Four Different Surface Sites[a] on Some Stable Faces of Benzamide. (A) Benzoic Acid in Syn-Planar Conformation (**3a**), (B) Benzoic Acid in Anti-Planar Conformation (**3b**), (C) *o*-Toluamide (**4a**), (D) *o*-Toluamide (**4b**), (E) *p*-Toluamide

face	E_l[b]	site[a]	A	B	C	D	E
(002)[c]	−52.4	1	12.0	6.0	8.9	43.6	52.8
		2	12.7	11.6	1.8	44.9	−1.3
		3	12.7	11.6	1.8	44.9	−1.4
		4	12.0	6.0	8.9	43.5	52.8
(10$\bar{2}$)	−38.6	1	12.4	6.0	6.4	44.9	53.1
		2	13.1	12.2	−0.2	0.6	−2.5
		3	13.3	12.2	−0.1	0.5	−2.6
		4	12.5	6.0	6.4	44.9	53.1
(100)	−37.3	1	13.0	6.5	6.7	45.2	53.0
		2	13.0	12.1	10.0	44.1	−2.5
		3	13.0	12.1	10.0	44.1	−2.6
		4	13.0	6.8	6.7	45.2	53.0
(10$\bar{4}$)	−33.8	1	13.6	11.6	−1.0	45.8	54.9
		2	13.4	12.1	8.9	0.2	53.6
		3	13.6	12.2	8.9	0.1	53.5
		4	13.7	11.6	−1.0	45.7	54.9
(011)	−31.6	1	10.3	10.0	6.0	45.5	53.3
		2	10.3	10.0	−1.4	46.3	41.5
		3	7.3	10.9	9.9	24.3	10.7
		4	7.3	10.9	9.5	23.8	53.5
(102)	−30.6	1	13.4	13.4	5.8	1.6	53.1
		2	12.9	12.8	9.8	44.0	−2.5
		3	12.8	12.8	9.8	44.0	−2.6
		4	13.5	13.5	5.9	1.6	53.1
(20$\bar{2}$)[c]	−29.7	1	13.4	12.5	−0.7	46.0	54.8
		2	12.8	6.3	10.0	44.1	−2.5
		3	12.8	6.3	10.1	44.0	−2.5
		4	13.5	12.5	−0.7	46.0	54.8
(202)[c]	−28.8	1	13.2	6.7	5.8	1.6	53.1
		2	12.9	12.2	10.0	44.2	−2.4
		3	12.9	12.1	10.0	44.1	−2.5
		4	13.5	6.7	5.8	1.6	53.1

[a] (1) x,y,z; (2) $-x,{}^1/_2 + y,{}^1/_2 - z$; (3) $-x,-y,-z$; (4) $x,{}^1/_2 - y,{}^1/_2 + z$. [b] $E_{cryst} = E_l + 2E_{att} = -64.4$ kcal/mol. [c] Halving of some layers is done because of space group symmetry $P2_1/c$.

The effect of the various additives on the crystal habit of benzamide was studied by energy calculations. The results are presented in Table IV, which summarizes the loss in energy in binding various additive molecules at the site of a substrate molecule on various benzamide faces. Benzoic acid[20] with a syn-planar conformation (**2a**) is most easily adsorbed at two surface sites on the {011} faces of benzamide with a loss of 7 kcal/mol. The change in attachment energy is maximal for this face (10 kcal/mol), suggesting that these faces should undergo the maximal increase in surface area. The {010} face, which can also adsorb benzoic acid with the syn-planar conformation, is not observed because it is not a stable face. The anti-planar (**2b**) conformer of benzoic acid should be most easily adsorbed on {101}, {10$\bar{1}$}, {001}, and {100}. Since this is not in agreement with the morphology of benzamide crystals grown in the presence of benzoic acid, this conformation of the additive can be ruled out.

o-Toluamide may adopt either one of the following molecular conformations (**4a**, **b**). The latter is clearly less stable, due to

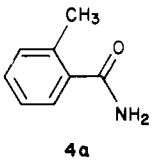

4a

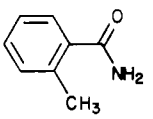

4b

intramolecular short contacts between the hydrogen atoms of the ortho methyl group and that of the amide group. The effect of both conformers, as additives, on the crystal habit of benzamide, was considered by energy calculations. The conformation of the additive was assumed to be similar to that of benzamide, except for the substitution of the relevant C–H bond by a C–CH_3 group. The results are summarized in Table IV.

o-Toluamide, in conformation (**4a**), was found to be most easily adsorbed at two molecular sites on {10*l*} faces such as {10$\bar{4}$}, in agreement with the experimentally observed large increase in the area of these faces. *p*-Toluamide is expected to bind on all {10*l*} faces and on {001}, which is the largest face. This prediction is compatible with the observation that thin {001} plates are obtained at very low concentrations of additive in solution and increasing amounts cause the deposition of powder.

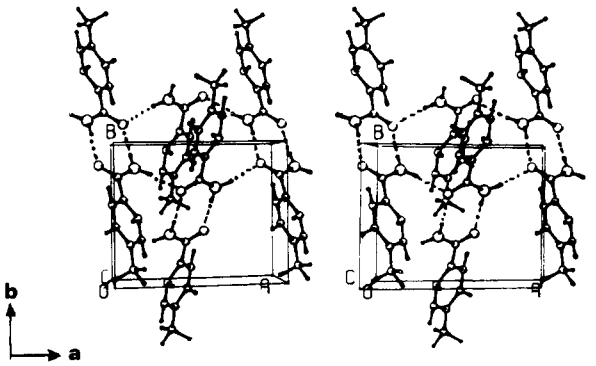

Figure 6. Packing arrangement of *p*-toluamide as viewed along the *c* axis.

1.3. *p*-Toluamide crystallizes from ethanol, in space group $P2_1/c$, as relatively thick {001} plates elongated in *a* and displaying well-developed side faces (Figure 7a).

In contrast to the previous cases in which the cyclic dimers forming the ribbon motif are related by a 5-Å translation, in the crystal of *p*-toluamide[22] the dimers are interlinked along an *a* glide to yield 001 layers. These layers juxtapose along the *c* axis by van der Waals interactions between tolyl groups (Figure 6). Thus, disruption of the hydrogen bonds between the dimers is expected in this case to affect growth in the *a* direction. Indeed *p*-toluic acid as the additive yields crystals extended in *b* (Figure 7b).

Cyclohexylamide inhibits the growth along the *c* direction due to steric hindrance exercised by the nonplanar cyclohexyl group

(22) Frolow, F., unpublished results.

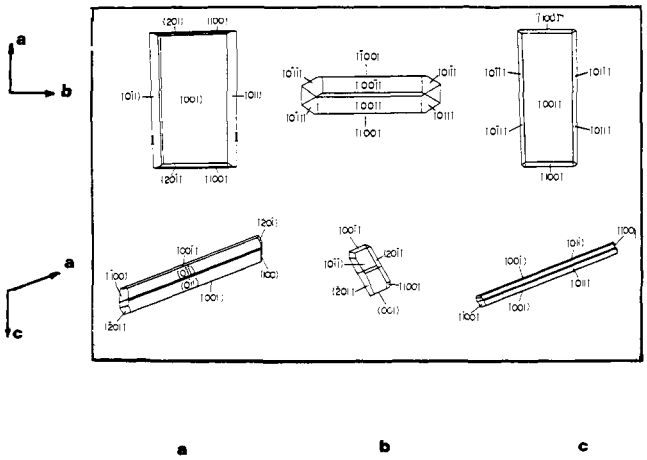

a b c

Figure 7. Crystals of *p*-toluamide grown in the absence and presence of additives, viewed along the *c* and *b* axis, respectively: (a) pure; (b) + *p*-toluic acid; (c) + cyclohexylamide.

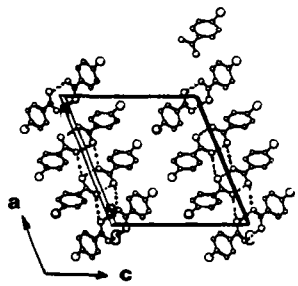

Figure 8. Packing arrangement of the α form of *p*-chlorobenzamide as viewed along the *b* axis.

of the additive. This induced separation of thin platelets extended in *a* (Figure 7c).

Inhibition of growth in the *b* direction was anticipated to be achieved by *p*-chlorobenzamide as the additive. However, this additive did not induce any significant change in habit of *p*-toluamide crystals, presumably because there is no difference in volume between substrate and additive.

1.4. *p*-Chlorobenzamide is dimorphic at room temperature. The α form (space group $P1$) crystallizes from ethanol in the form of large prisms, with prevalent faces {001}, {01$\bar{2}$}, and {20$\bar{1}$}.

Crystallization in the presence of small amounts of *p*-chlorobenzoic acid yields bars, extended in *b*. The effect of the additive is again understood from the host packing arrangement[23] (Figure 8).

The crystal contains one centrosymmetric dimer and two independent molecules which form a pseudocentrosymmetric dimer. These dimers are interlinked through NH···O hydrogen bonds along *a*. Substituting an amide molecule by the acid analogue in the syn-planar conformation (**2a**) results, as expected, in a repulsive interaction between O(hydroxyl)···O(amide), which disturbs the growth in the *a* direction.

1.5. *p*-Aminobenzamide crystallizes from aqueous solution, in space group $P2_1$, in the form of thin {100} rhombs with {011} side faces (Figure 10a).

In the crystal of *p*-aminobenzamide,[24] the molecules do not form H-bonded dimers, but a ribbon motif is formed from hydrogen bonding between molecules related by a twofold screw axis along *b*. The adjacent ribbons make contact along the *c* axis, bringing the *p*-amino group into juxtaposition with the NH_2 moiety of the amide group (Figure 9).

Introduction of *p*-aminobenzoic acid as the additive induces the separation of crystals with newly developed {102} faces, which

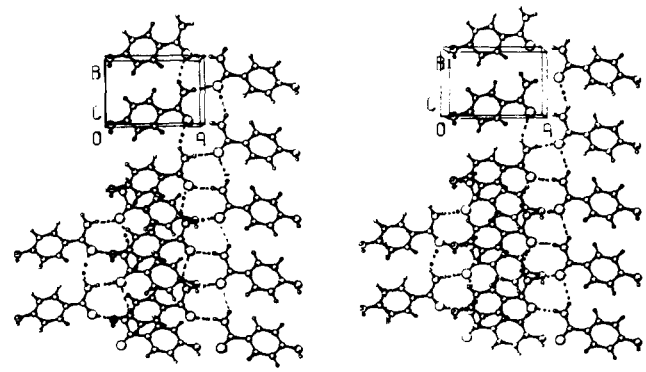

Figure 9. Packing of *p*-aminobenzamide as viewed along the *c* axis. For clarity, one *ab* layer is shown in the upper half of the picture and two in the lower one.

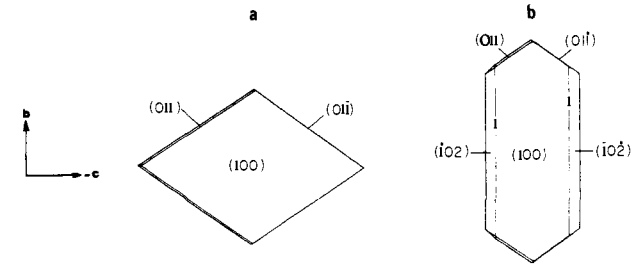

Figure 10. Crystals of *p*-aminobenzamide grown in the absence and presence of additive, viewed along the *a* axis: (a) pure; (b) + *p*-aminobenzoic acid.

Scheme II

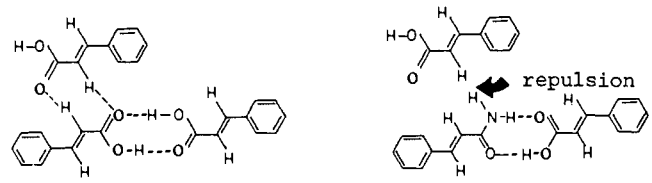

a b

are the result of hindrance of growth in the *c* direction (Figure 10b).

Unlike the previous examples, O(hydroxyl)···O(amide) repulsion along the 5-Å *b* axis, consistent with a syn-planar conformation (**2a**) of the additive carboxylic acid, cannot account for the observed change in crystal habit; O···O repulsion along the *a* axis, arising from an anti-planar conformation (**2b**), cannot explain the observed change in morphology either. Nevertheless, it is possible to present a plausible explanation for the change in crystal habit; replacement of an amide group by a carboxyl group, with a syn-planar conformation, would introduce repulsion between the O(hydroxyl) and the O(amide) along the *b* axis. This repulsion could be relieved by rotation of the carboxyl group about the exocyclic C–C bond, which would bring the O(hydroxyl) lone pair in a repulsive contact with the lone pair electrons of the amino group of the adjacent layer along the *c* axis, thus inhibiting growth in this direction. The carboxyl group would have to rotate in such a direction so as to decrease the torsion angle between the phenyl and carboxyl groups. Analogous rotations of the corresponding acid additives in the previously presented cases would be more difficult because in these structures the hydrogen-bonded cyclic dimers are more tightly interlinked along short translational axes of approximately 5 Å.

2. Carboxylic Acids. 2.1. (*E*)-Cinnamic acid is dimorphic. The α form (space group $P2_1/c$) is obtained from ethanol in the form of thin {010} plates (Figure 12a). Within the crystal, hydrogen-bonded cyclic dimers extended in *c* are interlinked by C–H(vinyl)···O(carbonyl) interactions predominantly along the

(23) Taniguchi, T.; Nakata, K.; Takaki, Y.; Sakurai, K. *Acta Crystallogr., Sect. B* **1978**, *B34*, 2574.

(24) Alleaume, M. Thesis. Bordeaux, 1967.

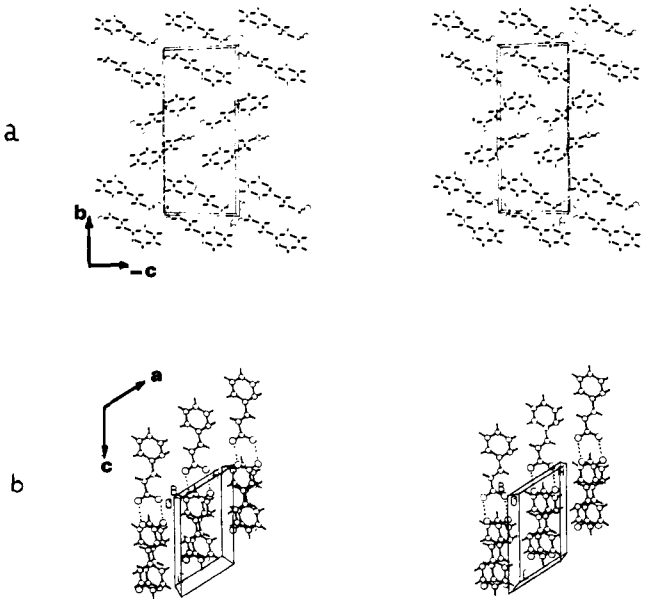

Figure 11. Packing arrangement of (*E*)-cinnamic acid (a) as viewed along the *a* axis and (b) as viewed along the *b* axis.

a axis (Scheme IIa), thus generating 010 layers. Juxtaposition of these layers by weak van der Waals interactions along *b* yields the observed {010} plates (Figure 11).[25]

Several additives were predicted to influence growth along *a* by disruption of the CH···O interactions within an 010 layer. In contrast to cinnamic acid, cinnamide invariably adopts a syn-planar —C=C—C=O conformation. Thus, replacement of cinnamic acid (Scheme IIb) would induce a repulsive CH···HN(amide) interaction, hindering growth along *a*.

A similar morphological change is expected for the additive *α*-chlorocinnamic acid, due to the C-Cl···O repulsion. *β*- and *o*-chlorocinnamic acid[19] are expected to affect crystal morphology in the same direction, because of unfavorable steric contacts. In fact, all four additives cause a relative increase in morphological importance of the {100} faces (Figure 12b and c), together with an increase in size of the side faces ($\bar{1}\bar{1}1$), ($\bar{1}11$), ($1\bar{1}\bar{1}$), and ($11\bar{1}$). This is easily explained, because the vectors along the direction of the CH···O intralayer interactions have a significant component normal to these faces as well.[26]

2.2. Benzoic acid crystallizes from petroleum ether/acetone, in space group $P2_1/c$, in the form of bars extended along *b* (Figure 14a).

Benzoic acid molecules form almost coplanar hydrogen-bonded dimers stacked in ribbons along *b*. These ribbons are held together by CH···O interactions. These combined ribbon and stack motifs generate 001 layers, which are juxtaposed by van der Waals interactions[27] (Figure 13).

Introduction of benzamide is expected to have an effect in the *b* direction. Unlike benzoic acid, which is a planar molecule, the stable conformation of benzamide is twisted by approximately 14° between the planes of the amide and the phenyl moieties.[16] This twist originates from the steric repulsion between the ortho hydrogens of the phenyl ring and the amide hydrogen atom. Benzamide, when bound to the benzoic acid crystal faces, should therefore inhibit growth along the stack axis *b*. Benzoic acid crystals, obtained with this additive, indeed show a significant change in habit in the *b* direction (Figure 14b).

It was observed as well that picolinamide (**5**), which is a planar amide molecule, does not inhibit growth along the stack axis *b*.

(25) Bryan. R. F.; Freyberg, D. F. *J. Chem. Soc., Perkin Trans. 2* **1975**, 1835.

(26) *p*-Chlorocinnamic acid, which is expected to hinder growth in the *c* direction as a result of steric hindrance, induced crystallization of solid solutions of the cinnamic acid in the *p*-chlorocinnamic acid crystal.

(27) Sim, G. A.; Robertson, J. M.; Goodwin, T. H. *Acta Crystallogr.* **1955**, *8*, 157.

Table V. Benzoic Acid: Layer Energy (E_l, kcal/mol) and Differences in Binding Energy (E_b, kcal/mol) and in Attachment Energy (E_{att}, kcal/mol) of Benzamide Molecule Inserted at Each of the Four Different Surface Sites[a] on Some Stable Crystal Faces. (A) Benzamide in a Hypothetical Planar Conformation, (B) Benzamide in Twisted Conformation (Φ = 20°)

			A		B		C	
face	E_l	site[a]	ΔE_b	ΔE_{att}	ΔE_b	ΔE_{att}	ΔE_b	ΔE_{att}
(002)[b]	−39.9	1	−0.1	0.0	1.3	0.0	1.3	8.6
		2	−0.1	0.0	1.6	0.0	9.2	0.5
		3	0.3	0.0	1.6	0.1	8.7	0.6
		4	−0.1	0.0	1.3	0.1	1.7	8.9
(100)	−29.3	1	−0.3	0.1	0.3	1.0	−0.5	10.4
		2	−0.5	0.3	1.2	0.5	8.9	0.7
		3	−0.3	0.5	1.1	0.5	7.7	0.7
		4	−0.2	0.1	0.4	1.0	0.0	10.6
($10\bar{2}$)	−29.8	1	−0.8	0.6	0.3	1.1	6.9	3.0
		2	−0.3	0.1	0.8	0.8	8.5	1.2
		3	−0.3	0.4	0.8	0.8	7.3	1.0
		4	−0.8	0.7	0.3	1.0	7.3	3.3
($20\bar{2}$)[b]	−25.2	1	0.1	0.3	0.5	0.8	−0.9	10.8
		2	0.7	−0.8	0.7	0.9	8.2	1.4
		3	0.9	−0.7	0.7	0.9	7.1	1.2
		4	0.2	0.3	0.6	0.8	−0.4	11.0
(011)	−19.1	1	0.3	0.5	1.8	0.5	−0.1	9.9
		2	−2.0	1.8	0.5	2.2	12.0	−2.4
		3	0.3	0.1	1.6	0.0	7.0	1.4
		4	−2.0	2.0	−1.2	2.6	12.5	−1.9

[a] (1) x,y,z; (2) $-x,-y,-z$; (3) $-x,{}^1/_2+y,{}^1/_2-z$; (4) $x,{}^1/_2-y,{}^1/_2+z$. [b] Halving of some layers is done because of space group symmetry $P2_1/c$.

Table VI. Strongest Intermolecular Interactions (kcal/mol) in Benzoic Acid Crystal. (A) Substrate/Substrate Interactions, (B)-(D) Substrate/Additive Interactions, (B) Additive Is a Planar Benzamide (Φ = 0°), (C) Additive Is a Twisted Benzamide with ϕ = 14°, (D) Additive Is a Twisted Benzamide with ϕ = 20°

neighbor					
site[a] $a_1a_2a_3$	sym-metry[b]	A	B	C	D
000	2	−7.2	−8.7	−8.7	−8.7
$0\bar{1}0$	1	−6.1	−5.7	−6.0	−6.7
010	1	−6.1	−5.9	−5.5	−2.8
010	2	−4.8	−4.6	−5.1	−6.8
100	1	−3.7	−4.1	−3.4	−1.2
$\bar{1}00$	1	−3.7	−4.7	−4.4	−5.2
$1\bar{1}0$	3	−2.0	−2.0	−1.8	−1.8
100	3	−2.0	−2.1	−2.4	5.3
110	2	−1.9	−2.0	−1.4	0.6

[a] The site of the neighboring molecule is described by the lattice vector $V = a_1a + a_2b + a_3c$ and the space group symmetry operator.[b] [b] (1) x,y,z; (2) $-x,-y,-z$; (3) $-x,{}^1/_2+y,{}^1/_2-z$; (4) $x,{}^1/_2-y,{}^1/_2+z$.

The effect of benzamide on benzoic acid crystal habit was studied by energy calculations. The conformation of benzamide adsorbed at the benzoic acid crystal faces is not uniquely defined.

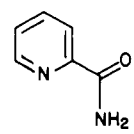

5

The torsion angle (Φ) between the planes of the phenyl ring and the carbonamide group may vary from 14° to 25°. The former was deduced to be a stable conformation of benzamide in the gas phase;[16] the latter, which was observed in the crystal structure of benzamide, was accounted for by the requirements of the H-bonding arrangement in this crystal.[15a] In the calculations of the effect of benzamide as the additive, we checked various conformations of the amide molecule in the range $-25° < \Phi < 25°$.

A planar benzamide molecule (Φ = 0°), which was used in the calculation to simulate the effect of a planar amide additive, is

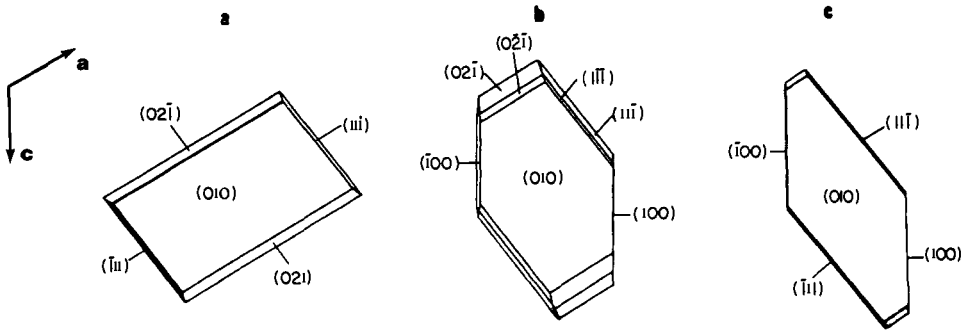

Figure 12. Crystals of (*E*)-cinnamic acid grown in the absence and presence of additives, viewed along the *b* axis: (a) pure; (b) + (*E*)-cinnamide or *α*- or *β*-chloro-(*Z*)-cinnamic acid; (c) + *o*-chlorocinnamic acid.

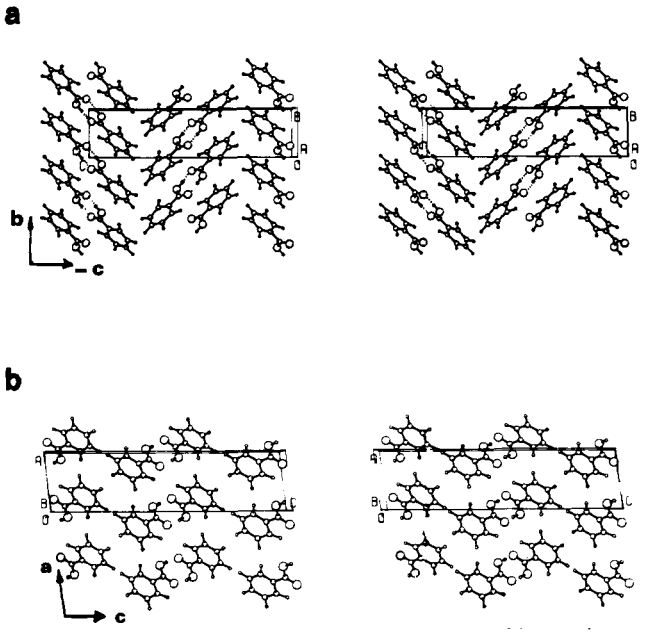

Figure 13. Packing arrangement of benzoic acid (a) as viewed along the *a* axis and (b) as viewed along the *b* axis.

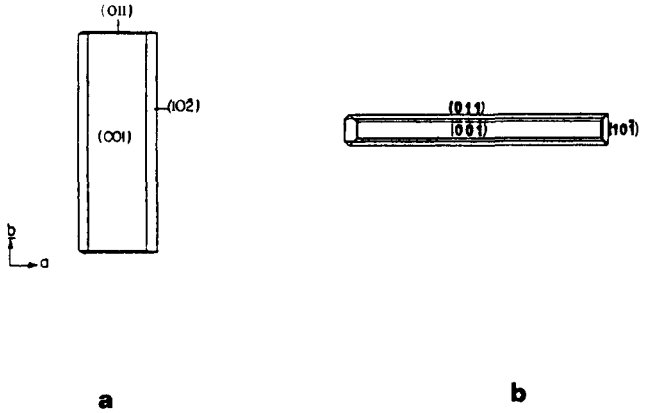

Figure 14. Crystals of benzoic acid grown in the absence and presence of additive, viewed along the *c* axis: (a) pure; (b) + benzamide.

expected to bind, with almost the same ease, at all the stable faces of benzoic acid (Table V). Moreover, the change in E_{att}, which measures the inhibition of growth by the adsorbate, is very low for all faces, and thus the overall habit of the crystal is not expected in this case to undergo any significant morphological modification. Benzamide with $\Phi = 14°$ was found to be most easily adsorbed on {011} faces, though the loss in binding energy in adsorbing this additive on other benzoic acid crystal faces is not as pronounced as in the other systems which were studied by this method (Tables II, IV, and V). Comparing substrate/substrate and substrate/additive intermolecular interactions for various conformations of the additive benzamide molecule (Table VI), it was found that planar benzamide ($\Phi = 0°$) or twisted additive with $\Phi = 14°$ does not introduce unfavorable intermolecular interactions at the site of adsorption, and the possibility that benzamide adopts a conformation with $\Phi > 20°$ or $\Phi < 0°$ is ruled out because these additives introduce unfavorable intermolecular interactions in the benzoic acid crystal.

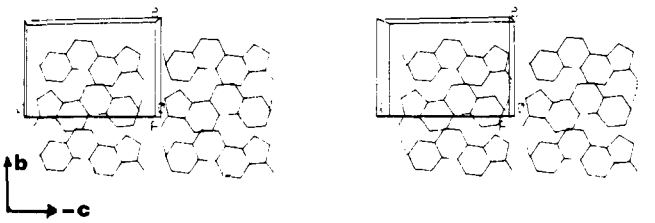

Figure 15. Packing arrangement of androsterone viewed along the *a* axis.

3. Steroids. 3.1. Androsterone (5-*α*-androstan-3-*α*-ol-17-one) (**6a**) crystallizes from ethyl acetate, in the polar space group $P2_1$, in the form of hexagonal thick {001} plates, delineated by faces {110}, {1$\bar{1}$0}, {100}, and {$\bar{1}$01} (Figure 16a).

Androsterone molecules, related by a twofold screw axis, are interlinked via hydrogen bonds between the 3-*α*-hydroxyl and the 17-keto groups, forming stacks along *b*. The molecules lie parallel

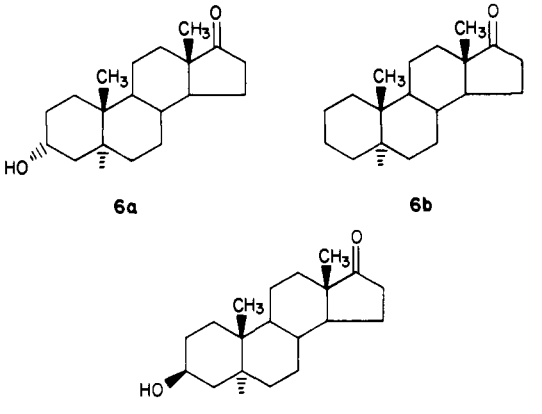

to the *bc* plane, but the OH···O hydrogen bonds are almost perpendicular to the {110} faces. The stacks of hydrogen-bonded molecules are connected along *c* and *a* by van der Waals interactions[28] (Figure 15).

The crystal is polar, and all hydrogen bonds are oriented in the same direction of the polar *b* axis, so that faces at the +*b* side have hydroxyl groups emerging at the surface, while faces at the −*b* side contain carbonyl groups. Introduction of additives which disturb the hydrogen-bonding pattern is expected therefore to influence differently the growth of the crystals at the two opposite ends of the polar *b* axis, depending on whether the hydrogen donor or acceptor group of the molecule has been modified.

(28) High, D. F.; Kraut, J. *Acta Crystallogr.* **1966**, *21*, 88.

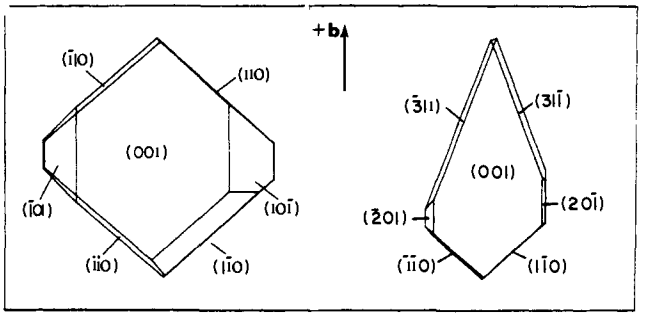

a b

Figure 16. Crystals of androsterone grown in the absence and presence of additive, viewed along the *c* axis: (a) pure; (b) + additive (**6b**).

Table VII. Androsterone: Layer Energy (E_l, kcal/mol), Attachment Energy (E_{att}), and Differences in Binding Energy (E_b, kcal/mol) and in E_{att} (kcal/mol) of Androstane Derivative (**6b**) Inserted at Each of the Two Different Surface Sites[a] on Some Stable Crystal Faces

face	E_l	E_{att}	site[a]	ΔE_b	ΔE_{att}
(001)	−54.2	−10.5	1	4.6	0.2
			2	5.0	−0.2
(10$\bar{1}$)	−47.5	−13.9	1	5.0	−0.1
			2	5.0	−0.2
(100)	−46.7	−14.3	1	4.7	0.1
			2	5.1	−0.3
(101)	−36.9	−19.2	1	4.6	0.3
			2	5.1	−0.3
(1$\bar{1}$0)	−31.8	−21.7	1	3.9	1.0
			2	4.6	0.3
(110)	−31.8	−21.7	1	0.4	4.5
			2	4.6	0.2
(11$\bar{1}$)	−29.8	−22.7	1	0.7	4.2
			2	4.8	0.0
(1$\bar{1}$1)	−29.8	−22.7	1	4.0	0.9
			2	4.7	0.1
(011)	−27.3	−24.0	1	0.7	4.2
			2	4.6	0.2

[a] (1) x,y,z; (2) $-x,{}^1/_2+y,-z$.

Crystals grown in the presence of 5-α-androstan-17-one (**6b**), lacking the OH group at the C(3) position, appear as {001} plates elongated along *b* and delineated by the new steep faces {311} in the +*b* direction, while the −*b* side remains delineated by {1$\bar{1}$0}, as in the pure crystal (Figure 16b). In this example, the effect of the additive consists of severing a hydrogen bond rather than creating further repulsion, as in the previous systems.[29]

According to energy calculations (Table VII) the additive may be adsorbed with minimal loss in energy at faces (110) and ($\bar{1}$10) but not at (1$\bar{1}$0) and ($\bar{1}\bar{1}$0). Once bound, it will hinder growth selectively in the +*b* direction, as is in fact observed. We cannot, however, justify in detail the formation of the steep {311} faces, which are not stable faces but are most probably composed of combinations of other stable faces forming microscopic steps.[30]

3.2. Epiandrosterone (5-α-androstan-3-β-ol-17-one) (**6c**) crystallizes from ethyl acetate, in space group $P2_1$, in the form of pentagonal crystals with polar morphology, displaying well-developed {0$\bar{1}$0} and {1$\bar{1}$0} faces at the negative side of the *b* axis and rounded faces at the positive side (grossly {170}) (Figure 18a).

Epiandrosterone molecules are elongated in *b* and interlinked by hydrogen bonds 3-β-OH···O=C(17), which are almost perpendicular to the (110) and ($\bar{1}$10) planes. The hydrogen-bonding pattern[31] is polar in the sense that all OH groups point toward

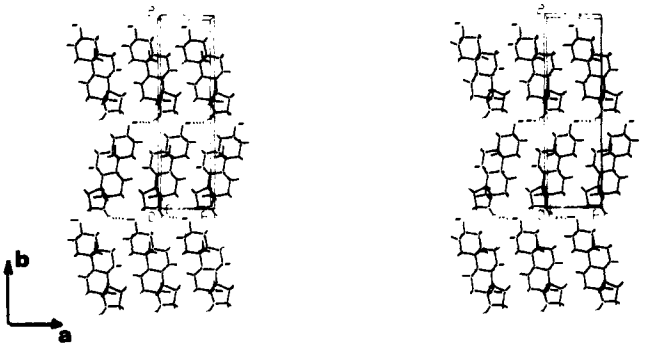

Figure 17. Packing of epiandrosterone viewed along the *c* axis.

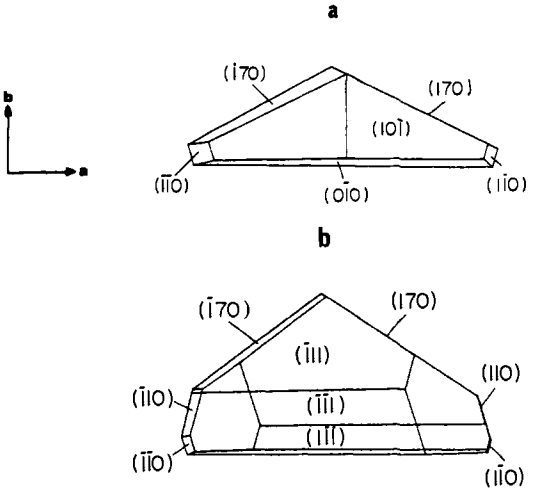

Figure 18. Crystals of epiandrosterone grown in the absence and presence of additive, viewed along the *c* axis.

+*b* and all keto groups toward ($\bar{1}$10) (Figure 17).

The additive 5-α-androstan-17-one (**6b**), lacking the 3-hydroxyl group, induces the appearance of faces (110) and ($\bar{1}$10) at the +*b* end of the polar axis (Figure 18). The effect is thus again qualitatively correct, since interruption of the hydrogen-bonded array of molecules at the site of the additive causes retardation of growth of (110) and ($\bar{1}$10) to which the additive is most easily bound.

Discussion

We have shown that the morphology of a crystal can be modified in a controlled way by appropriate crystal growth inhibitors which can bind at preselected faces, decreasing their growth rate relative to the pure crystal and to that of other unaffected faces. The inhibitor is a substrate molecule modified only at one position, which can conceivably occupy particular sites at the crystal surface and thereby disrupt specific intermolecular interactions. The direction of these interactions defines the faces whose growth is impaired. A face which is already expressed in the habit of the pure crystal may increase its morphological importance in the affected one to such an extent that it can become prevalent. Alternatively, new faces may develop. Faces which are not expressed in the pure crystal are of two main types: virtual faces which are stable, but grow too fast and thus do not appear in the habit of the unaffected crystal,[32] or faces which are not stable. The decrease in the growth rate, imposed by the inhibitor, may induce the appearance of faces of the first kind but not of the second. The stability of the various faces, expressed by their layer energies, is obtained by energy calculations, thus leading to more accurate predictions of morphological modifications.

We examined first systems in which the geometry of the guest molecule within the host lattice is unequivocally fixed, as, for

(29) The morphological studies of androsterone were complicated by the appearance of crystals of a second polymorph, which was found to be a hydrate of space group $P2_1$.[22]

(30) (a) Polar crystals tend to develop steep faces along the polar direction.[30b] (b) Curtin, D., private communication.

(31) Weeks, C. M.; Cooper, A.; Norton, D. A. *Acta Crystallogr., Sect. B* **1971**, *B27*, 1562.

(32) Johnson, A., 1900, Wachstum und Auflosung der Kristalle, Leipzig, Wilh. Euglemann.

example, cinnamic acid in cinnamide or in the case of the rigid steroids. In these systems, the change in crystal morphology was always foreseen. We have here systematically applied the above principles to various substrates of different nature like primary amides, carboxylic acids, and steroids. Furthermore, morphological modifications of various α-amino acid crystals have been performed in the past by using the same methods.[4-6] Other analogous examples of habit modification were studied already in the mid 1960s in sugar chemistry, in connection with the important problem of sugar purification. For example, various trisaccharides were reported to affect the habit of sucrose,[33] and other sugars, particularly β-lactose, have a dramatic effect on the crystallization of α-lactose.[34]

Since all these examples fit within the same framework, it is clear that the phenomenon of morphological modification is general and subject to well-defined and predictable rules. Consequently, we are now able to reverse roles and exploit the observed morphological changes in order to elucidate fine intermolecular interactions between the additive and substrate inside the host crystal. For example, from the effect of acids inside amide crystals, we glean information on O···O repulsion (section 1) and from that of bulky Cl or methyl substituents instead of hydrogen we learn about steric hindrance.

The modified habit may also serve as an experimental way of establishing the conformation of the additive[35] and provide limits for energy barriers which may or may not be overcome by crystal forces, e.g., cinnamide in cinnamic acid, *N*-methylcinnamide in cinnamide, or benzamide in benzoic acid crystals. The additive cinnamide assumes a syn-planar conformation in the host (*E*)-cinnamic acid, which tends to assume an anti-planar C=C—C=O conformation. *N*-Methylcinnamide adopts a syn-planar O=C—N—CH_3 conformation in the host cinnamide. The experimental results on the effect of benzamide and picolinamide on the benzoic acid crystal habit serve as a probe for establishing the most favorable conformation of the benzamide additive. The substrate benzoic acid is planar whereas the adsorbed benzamide molecule must be distorted due to intramolecular H···H repulsion. The best agreement between the lattice energy calculations, the conformational requirements and the experimental results is for a twist of 14° between the amide group and the phenyl ring. This value is in excellent agreement with the value deduced for benzamide by packing analyses.[15,16] An opposite tendency was deduced in the host/additive system *p*-aminobenzamide/*p*-aminobenzoic acid; the adsorbed additive tends to be planar, in contrast to the substrate molecule.

We have investigated a number of systems in which the additives were obtained by modifying two different parts of the substrate molecule. In a general way it can be stated that a combined effect is observed only when the two modifications do not prevent adsorption of the guest molecule at specific surfaces of the host crystal. Thus, α-chlorocinnamic acid affects cinnamide crystal habit, because the molecule may be adsorbed on the {010} and {011} faces with both the hydroxyl oxygen lone pair and the α-Cl substituent pointing away from the crystal interior. On the other hand, β-chlorocinnamic acid does not affect cinnamide crystal habit, because the two modified sites of the additive, with respect to the substrate, would affect the $+b$ and $-b$ directions simultaneously, thus preventing the molecule from being adsorbed at either end of the ribbon motif. *p*-Chlorocinnamic acid induces on cinnamide a combination of two separate effects in the *a* and *b* directions, as induced by *p*-chlorocinnamide and cinnamic acid, respectively (section 1.1). The smaller extent of the combined effect, however, reflects the increased difficulty in adsorption. In an analogous way it was observed that succinic acid (**7c**) does not have any effect on succindiamide (**7b**) crystal habit, because the two OH oxygen lone pairs point in opposite directions. Succinamic acid (**7a**), on the other hand, affects crystal growth of succindiamide in the expected direction of the intermolecular NH_a···O=C hydrogen bond of the latter, which is replaced by an O···O repulsion at the site of the additive. This deduction is consistent with calculations performed on these systems.[36] It is expected that a similar behavior will be observed when various aliphatic diacid additives are added to the corresponding aliphatic diamides; all members with an even number of carbon atoms akin to (**7c**) in which the two oxygen lone pairs of the adsorbed acid additive would create repulsion in two opposite directions (by virtue of the molecular center of symmetry) should not be absorbed. However, for aliphatic diamide substrates (**8a**) with an odd number of carbon atoms, in which both amide H_a atoms form hydrogen bonds in the same direction (by virtue of a molecular twofold axis), the corresponding diacids (**8b**) should be adsorbed and cause morphological modification.

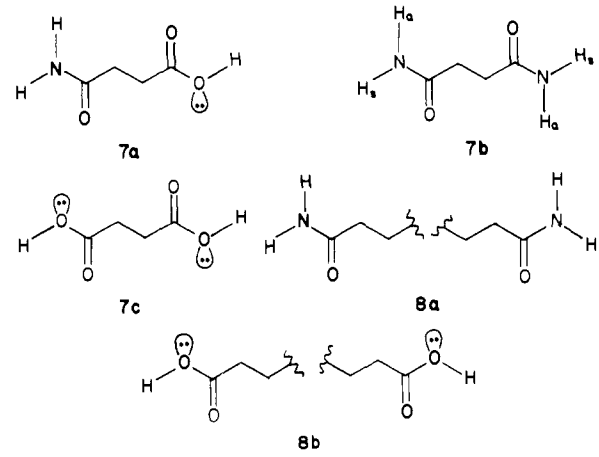

Important information concerning the nature of substrate–additive interactions can be gleaned from the occluded additive. The amount of occluded inhibitor is related to the loss in binding energy at the site of the occlusion. Thus, up to 3% of *p*-chlorocinnamide was found inside cinnamide crystals because the guest molecule is incorporated in the hydrogen-bonded ribbon motif exactly as the substrate molecule and interferes only with the relatively weak van der Waals interactions between layers. In contrast, cinnamic acid is occluded in a maximum amount of 0.5%. This is explained by the large loss in energy due to the binding of the additive molecule instead of substrate, the formation of an acid/amide hydrogen-bonded dimer, which is less stable by 4 kcal/mol than the amide/amide dimer, the disruption of a hydrogen bond of 6 kcal/mol, and the introduction of an O···O repulsion, calculated to be of 1–2 kcal/mol. On the other hand, almost 20% of aspartic acid was found occluded in the crystal of asparagine·H_2O, despite a similar absolute loss in energy.[2] This is explained by the fact that asparagine is interlinked to its neighbors by several strong hydrogen bonds, only one of which is replaced by O···O repulsion at the site of the additive. The relative loss in energy is thus low in this system, in contrast to cinnamic acid in cinnamide. The large amount of occluded aspartic acid allowed us in this last system to map its position in the crystal lattice and to confirm the geometry of the contact resulting from O···O repulsion.[18]

The mechanism of additive occlusion implies that the guest is not randomly distributed within the substrate crystal but rather occupies specific sites, depending on the faces through which it was incorporated into the crystal. For example, in the case of cinnamide/cinnamic acid, it is evident from Scheme I and from Table I that the acid molecule can occupy only one out of the two centrosymmetrically related sites: site 1 when occluded from the $+b$ end and site 2 from the $-b$ end. This selective occlusion must be associated with reduction in crystal symmetry from centrosymmetrical $P2_1/c$ to two chiral $P2_1$ crystal halves of opposite

(33) (a) Smythe, B. M. *Aust. J. Chem.* **1967**, *20*, 1115. (b) van Hook, A. *Krist. Acad. Nauk SSSR Inst. Kristallogr.* **1968**, *8*, 45. (c) Mantovani, G.; Gilli, G.; Fagioli, F. *C. R. Assem. Comm. Int. Tech. Sucr., 13th* **1967**, 289.

(34) (a) van Kreveld, A.; Michaelis, A. S. *J. Dairy Sci.* **1965**, *48*, 259. (b) van Kreveld, A. *Neth. Milk Dairy J.* **1969**, *23*, 258.

(35) Weissbuch, I.; Berkovitch-Yellin, Z.; Lahav, M.; Leiserowitz, L. *Isr. J. Chem.*, in press.

(36) Berkovitch-Yellin, Z., unpublished results.

Table VIII. Crystallization Conditions

material	solvent	concn, mg/mL	method	add concn % w/w
(*E*)-cinnamide	ethyl acetate	35	slow cooling	10
benzamide	ethanol	240	slow evap	10, 5, 3
p-toluamide	ethanol	100	slow evap	10
p-clorobenzamide	ethanol	120	slow evap	10
p-aminobenzamide	water	20	slow evap	10
(*E*)-cinnamic acid	ethanol	160	slow evap	10
benzoic acid	petroleum ether/acetone	10	slow evap	10
androsterone	ethyl acetate	25	slow evap	25
epiandrosterone	ethyl acetate/petroleum (6:1)	28	slow evap	20

handedness. Direct evidence for this hypothesis has been provided by the enantiomeric segregation of occluded α-amino acid additives into the crystals of α-glycine[6] and (*R*,*S*)-serine.[5]

A consequence of this analysis is that systems of solid solutions which are chemically and thermodynamically very similar may in fact display different extents of solid miscibilities, depending upon the symmetry of the growing crystal face. Thus, the structure and the extent of solid solubility may be a kinetically controlled surface phenomenon, as well as a thermodynamical bulk phenomenon.

Experimental Section

Materials were prepared by conventional methods. They were purified by liquid chromatography followed by multiple recrystallizations from doubly distilled solvents, and their purity was checked by HPLC. The analyses of the amounts of additive occluded inside the substrate crystals were performed by HPLC (column 250 × 4 mm, Nucleosil 10 C18, 10 μm), using as eluent 0.05 M acetate buffer, pH 4, 40% in methanol, on a liquid chromatograph, Waters Assoc., equipped with UV detection (254 nm).

Crystallization Conditions. Appropriate conditions for crystallization of the various pure compounds were first determined such that the crystals formed are homogeneous and reproducible with respect to their morphology. This means that at least 90% of the crystals have the same habit. The affected crystals were grown in parallel under exactly the same conditions. Inhibitors were dissolved into the supersaturated solution of the substrate before the onset of crystallization. The definition of typical habit of the affected crystal follows the same criteria as for the pure compound. The habit and morphology of typical pure and affected crystals were determined on a Siemens X-ray diffractometer[37] and compared. The new faces which develop in the affected crystals, or those which substantially increase in their surface area, relative to the other faces, are referred to as affected faces. Crystallizations were performed in the conditions specified in Table VIII from 10 to 25 mL batches of solution in 25–50 mL Erlenmeyers, at room temperature. (*E*)-Cinnamide was crystallized in a thermostat over a temperature gradient 60–30 °C, lowering the temperature 2 °C/day. All data are the result of many multiple sets of experiments.

Acknowledgment. We thank the Israel Academy of Science and Humanities, the US-Israel Binational Foundation, Jerusalem, and the donors of the Petroleum Research Fund, administered by the American Chemical Society, for financial support of this work. One of us (L.A.) is the recipient of the Helena Rubinstein Career Development Chair. We thank Rachel Yerushalmi for assisting in the growth of some of the crystals.

Registry No. (*E*)-Cinnamide, 22031-64-7; (*E*)-cinnamic acid, 140-10-3; (*E*)-*o*-chlorocinnamide, 95422-22-3; (*E*)-*p*-chlorocinnamide, 36650-34-7; (*Z*)-β-chlorocinnamide, 95422-23-4; (*Z*)-α-chlorocinnamide, 74305-85-4; benzamide, 55-21-0; *o*-toluamide, 527-85-5; *p*-toluamide, 619-55-6; benzoic acid, 65-85-0.

(37) Coppens, P.; Leiserowitz, L.; Rabinovitch, D. *Acta Crystallogr.* **1965**, *18*, 1035.

Kinetics and Mechanism of Substitution Reactions of Some (η^3-Allyl)manganese Tetracarbonyl Compounds

G. Todd Palmer and Fred Basolo*

Contribution from the Department of Chemistry, Northwestern University, Evanston, Illinois 60201. *Received October 4, 1984*

Abstract: Kinetic data are reported for CO substitution of (η^3-C_3H_4X)$Mn(CO)_4$, where X is a substituent in the 1- or the 2-position of the allyl ligand and where X^1 = H, Me, Ph, *t*-Bu, and Cl. Also the *anti*- and the *syn*-(η^3-C_3H_3(1,2-Ph_2))$Mn(CO)_4$ isomers were prepared for the first time and their rates of substitution determined. In all cases the rates of reaction are first order in substrate concentration and zero order in entering nucleophile concentrations. Studies on decarbonylation reactions of (η^1-C_3H_5)$Mn(CO)_4L$ rule out an $\eta^3 \rightarrow \eta^1 \rightarrow \eta^3$ mechanism. It appears that CO substitution takes place by a dissociation (S_N1) process, and the kinetic parameters for (η^3-C_3H_5)$Mn(CO)_4$ are k(45 °C) = 2.8 × 10^{-4} s^{-1}, ΔH^* = 26.8 kcal/mol, and ΔS^* = 9.6 eu. Substituents on the 1-position of the allyl group have a small retardation effect on the rates of CO substitution. Substituents on the 2-position enhance the rates of reaction; furthermore, this rate enhancement increases with increasing bulkiness of the substituent. Still, the maximum rate observed was only 500 times greater than that for the parent compound, and this is for the 2-*tert*-butylallyl compound. Unfortunately, all attempts to prepare the desired compounds with strong electron-donating and -withdrawing substituents on the allyl ligand failed.

There has been much interest in η^3-allyl organometallic complexes,[2] since it was first demonstrated[3] in the late 1950's that (C_4H_7)$Co(CO)_3$ has an η^3-bonding configuration. Kinetic studies[4] on carbonyl-substitution reactions of (η^3-C_3H_5)$Co(CO)_3$ (eq 1)

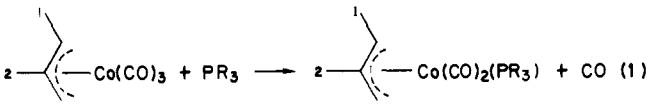

(1) Abbreviations: A = absorbance, *n*-Bu = *n*-butyl, *t*-Bu = *tert*-butyl, Cy = cyclohexyl, Et = ethyl, k_{obsd} = observed rate constant, Me = methyl, NBS = *N*-bromosuccinimide, Ph = phenyl, ΔH^* = enthalpy of activation, ΔS^* = entropy of activation.

0002-7863/85/1507-3122$01.50/0